Electrical detection of single magnetic skyrmion at room temperature

Riccardo Tomasello, Marco Ricci, Pietro Burrascano, Vito Puliafito, Mario Carpentieri, and Giovanni Finocchio

Citation: AIP Advances **7**, 056022 (2017); doi: 10.1063/1.4975998
View online: http://dx.doi.org/10.1063/1.4975998
View Table of Contents: http://aip.scitation.org/toc/adv/7/5
Published by the American Institute of Physics

Electrical detection of single magnetic skyrmion at room temperature

Riccardo Tomasello,[1] Marco Ricci,[1,a] Pietro Burrascano,[1] Vito Puliafito,[2] Mario Carpentieri,[3] and Giovanni Finocchio[4,a]
[1]*Department of Engineering, Polo Scientifico Didattico di Terni, University of Perugia, Terni I-50100, Italy*
[2]*Department of Engineering, University of Messina, I-98166 Messina, Italy*
[3]*Department of Electrical and Information Engineering, Politecnico di Bari, via E. Orabona 4, I-70125 Bari, Italy*
[4]*Department of Mathematical and Computer Sciences, Physical Sciences and Earth Sciences, University of Messina, Messina I-98166, Italy*

(Presented 3 November 2016; received 23 September 2016; accepted 11 November 2016; published online 8 February 2017)

This paper proposes a protocol for the electrical detection of a magnetic skyrmion via the change of the tunneling magnetoresistive (TMR) signal in a three-terminal device. This approach combines alternating spin-transfer torque from both spin-filtering (due to a perpendicular polarizer) and spin-Hall effect with the TMR signal. Micromagnetic simulations, used to test and verify such working principle, show that there exists a frequency region particularly suitable for this achievement. This result can be at the basis of the design of a TMR based read-out for skyrmion detection, overcoming the difficulties introduced by the thermal drift of the skyrmion once nucleated. [http://dx.doi.org/10.1063/1.4975998]

INTRODUCTION

Magnetic solitons[1–5] are fascinating particle-like magnetization textures with promising properties for the use in spintronic devices. Among them, skyrmions are attracting a large interest for their fundamental properties, such as topological protection,[6] and potential technological applications in racetrack memories,[7–9] oscillators,[10–13] detectors,[14] and logic gates.[15] The recent experimental evidences[16–19] that Néel skyrmions can be stabilized at room temperature in multilayers where a sufficient interfacial Dzyaloshinskii–Moriya interaction (i-DMI)[20,21] arises, and that they can be manipulated by the spin-transfer torque (STT) from the spin-Hall effect (SHE),[22–24] have been pushing the research towards the development of a skyrmion based technology.[25,26] Two key aspects for the skyrmion implementation in devices concern its nucleation and detection. For the former, while the experimental nucleation of skyrmions has been achieved by using external out-of-plane fields,[17–19] the control of the single skyrmion nucleation at room temperature is still an open challenge, although many numerical works have predicted it.[7,27–29] For the latter, skyrmions have been detected by different techniques, such as topological Hall effect,[6,30,31] Lorentz transmission electron microscopy,[32,33] spin-polarized tunneling microscopy,[34–36] polar magneto-optical Kerr effect microscope,[16] scanning transmission X-ray microscopy,[17,19] and photoemission electron microscopy combined with X-ray magnetic circular dichroism.[18] However, a suitable method to ensure an easier integration of skyrmionic devices in CMOS systems concerns a fully electrical detection of skyrmions. Recently, the tunneling non-collinear magnetoresistance[37] has been used, and many works have pointed out the possibility to use the tunnel magnetoresistance (TMR). The key issue is that the skyrmion, once nucleated at room

[a]email: marco.ricci@unipg.it and gfinocchio@unime.it.

temperature, is characterized by a thermal drift[38,39] because of the translational invariance which impedes the steady presence of the skyrmion below a magnetic tunnel junction (MTJ) read-head. To fix this problem, here we propose a detection protocol based on the TMR and SHE from a microwave current, as well as the combination of SHE and STT, in a three terminal device.[23,40–42] Such a system is composed of an MTJ with a perpendicular polarizer, built on top of a heavy metal strip, and allows one to control the magnetization dynamics in the MTJ free layer by means of two electrically independent currents: one flowing through the heavy metal (SHE), and the other one flowing through the MTJ (STT). The application of a microwave current drives continuously the skyrmion motion below the MTJ, leading to a dynamical change of the magnetoresistance signal linked to the out-of-plane component of the magnetization. This signal univocally indicates the presence of the skyrmion, and then, the successfully accomplishment of the nucleation process that can be, for instance, obtained by a dc STT as predicted in.[7]

MICROMAGNETIC MODEL AND DEVICE

The study is performed by means of a *state-of-the-art* processing tools and micromagnetic solver which numerically integrates the Landau-Lifshitz-Gilbert equation:[43–45]

$$(1+\alpha^2)\frac{d\mathbf{m_f}}{d\tau} = -(\mathbf{m_f}\times\mathbf{h_{eff}}) - \alpha\left[\mathbf{m_f}\times(\mathbf{m_f}\times\mathbf{h_{eff}})\right] - \frac{g\mu_B\theta_{SH}}{2\gamma_0 e M_S^2 t_{FL}}\left[\mathbf{m_f}\times(\mathbf{m_f}\times(\hat{z}\times\mathbf{j_{HM}}))\right]$$
$$+\frac{g\mu_B\theta_{SH}}{2\gamma_0 e M_S^2 t_{FL}}\left[\mathbf{m_f}\times(\hat{z}\times\mathbf{j_{HM}})\right] - \frac{g\mu_B\mathbf{j_{MTJ}}}{\gamma_0 e M_S^2 t_{FL}}\varepsilon_{MTJ}(\mathbf{m_f},\mathbf{m_p})\left[\mathbf{m_f}\times\left(\mathbf{m_f}\times\mathbf{m_p}\right) - q(V)\left(\mathbf{m_f}\times\mathbf{m_p}\right)\right] \tag{1}$$

where α is the Gilbert damping, $\mathbf{m_f}$ is the normalized magnetization of the MTJ free layer, and $\tau = \gamma_0 M_s t$ is the dimensionless time, with γ_0 being the gyromagnetic ratio, and M_s the saturation magnetization of the MTJ free layer. $\mathbf{h_{eff}}$ is the normalized effective field, which includes the exchange, magnetostatic, anisotropy and external fields, as well as the i-DMI[46,47] and thermal field.[48] g is the Landé factor, μ_B is the Bohr magneton, θ_{SH} is the spin-Hall angle, e is the electron charge, t_{FL} is the thickness of the ferromagnetic free layer, and $\hat{z}$ is the unit vector along the out-of-plane direction. $\varepsilon_{MTJ}(\mathbf{m_f},\mathbf{m_p}) = \frac{2\eta}{\left[1+\eta^2(\mathbf{m_f}\cdot\mathbf{m_p})\right]}$ is the polarization function, where η is the spin polarization factor, and $\mathbf{m_p}$ is the magnetization of the pinned layer, which is considered fixed for all the simulations. $q(V)(\mathbf{m_f}\times\mathbf{m_p})$ is the perpendicular torque term that depends on the voltage applied to the MTJ leads.[49]

We consider a three-terminal device composed of an ultrathin ferromagnetic layer in contact with a Pt heavy metal (HM), in order to achieve a large enough i-DMI and SHE. The ferromagnet acts as the free layer of the point contact MTJ deposited on top of it, which permits to apply a localized STT (see Fig. 1(a) for a sketch of the device, where a cartesian coordinate system has been introduced). The MTJ free layer has a 400x200 nm^2 elliptical cross section with thickness of 0.8 nm, and its major axis is oriented along the y-direction, in order to exploit the SHE-driven motion of the skyrmion along the direction perpendicular to the electrical current (x-axis).[8] The pinned layer has a fixed out-of-plane easy axis of the magnetization and it is patterned as a nano-contact.[12,14] The discretization cell used is 2.5x2.5x0.8 nm^3. In our simulations, we consider typical experimental systems (CoNi/Pt),[50] whose physical parameters are: $M_S = 600$ kA/m, $A = 20$ pJ/m, perpendicular anisotropy constant $k_u = 0.60$ MJ/m^3, $D = 3.0$ mJ/m^2, $\alpha = 0.1$, $\eta = 0.66$, and $\theta_{SH} = 0.1$.

RESULTS AND DISCUSSION

We analyze the skyrmion stability at room temperature $T = 300$ K in presence of an external normal-to-plane field $H_{ext} = 25$ mT. The skyrmion core[14] is along the negative z-direction. Statistical analyses (simulations 500 ns long) of the skyrmion diameter show that its mean value is around 40 nm, therefore we design the nanocontact to have a diameter of 50 nm in order to achieve a sufficiently large TMR signal when the skyrmion goes under it. Once the contact is fixed, we achieve the skyrmion nucleation by injecting a large enough dc current pulse through the MTJ.[7] After the current j_{MTJ} is

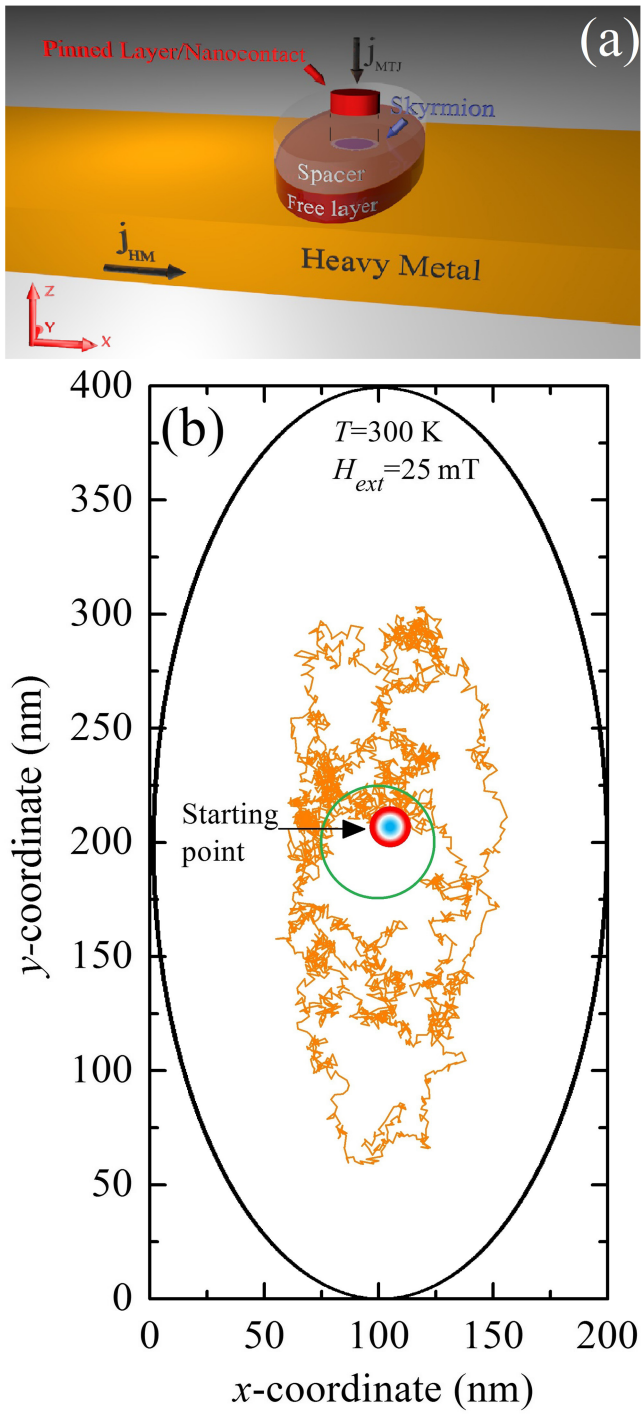

FIG. 1. (a) Schematic representation of the three-terminal device studied. (b) Trajectory of the skyrmion center at $T = 300$ K and for $H_{ext} = 25$ mT, when no microwave current is applied. The solid black line indicates the MTJ free layer under analysis, while the solid green line represents the region under the nanocontact.

switched off, the skyrmion does not remain under the nanocontact, because it is subject to thermal fluctuations that give rise to a breathing, shape deformations, as well as a Brownian drift,[38,39] as we can see in Fig. 1(b), where the trajectory of the skyrmion center is plotted (no microwave current is applied). The thermal drift of the skyrmion, even in presence of a confined ferromagnet, does

not allow one to detect it directly with a dc current flowing through a standard TMR read-head, because it is located most of the time out of the nanocontact region. We solve this issue by driving the skyrmion motion via a microwave current. In particular, we can use two independent currents in the three-terminal device, permitting the analysis of three configurations: (*i*) only SHE, (*ii*) only STT, (*iii*) combination of SHE and STT.

In the case (*i*), we apply an in-plane sinusoidal current $j_{HM}(t) = J_{HM}\sin(2\pi f_{HM} t)$ along the x-axis with amplitude J_{HM} = 30 MA/cm^2, frequency f_{HM} from 0.1 GHz to 1 GHz, and duration of 100 ns. For f_{HM}<0.3 GHz, the skyrmion is expelled from the free layer, entailing a detection failure. For 0.3 GHz$\leq f_{HM} \leq$0.7 GHz, the skyrmion starts to alternately shift along the y-axis.[8] In particular, by starting from the region under the nanocontact, the skyrmion moves towards the bottom edge in the semi-period when the current is negative, whereas it goes back towards the nanocontact when the current is positive. Each time that it passes below the nanocontact induces a variation of the out-of-plane component of the magnetization $<m_{z\_uc}>$ (see Fig. 2(a)), and, hence, of the TMR ($\propto (1 - \langle m_{z\_uc}\rangle)/2$). By injecting a subcritical dc current via the MTJ, it is possible to convert the oscillating resistance

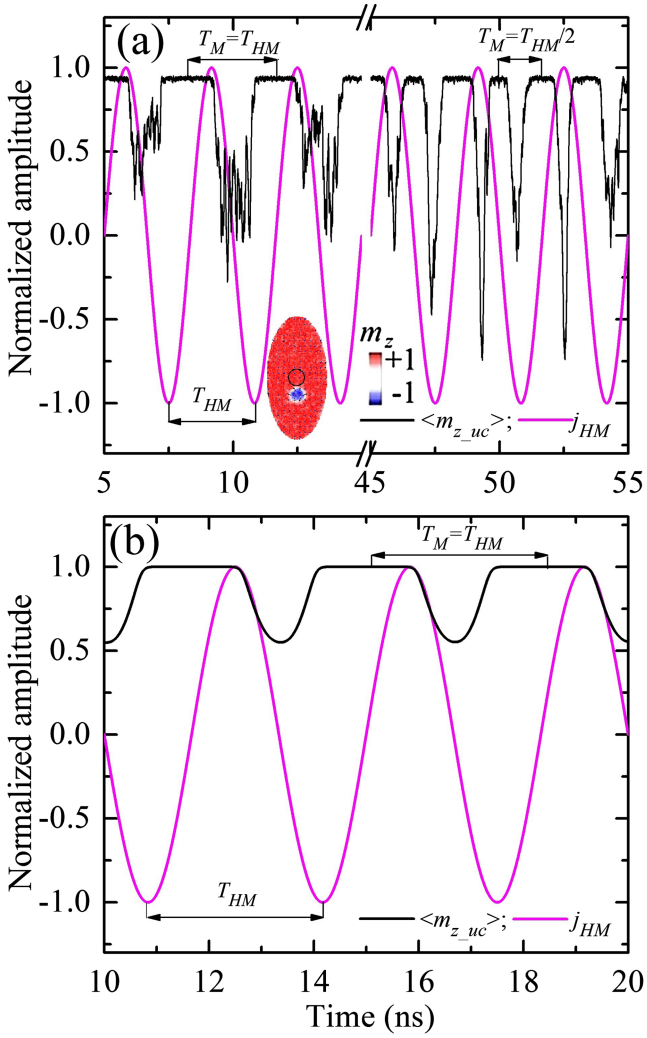

FIG. 2. Temporal evolution of the normalized z-component of the magnetization under the nanocontact (black curve) and the applied normalized microwave current (magenta curve) flowing in the heavy metal only (SHE), for H_{ext} = 25 mT at (a) T = 300 K and (b) T = 0 K. The current amplitude and frequency are 30 MA/cm^2 and 0.3 GHz, respectively. In (a), $<m_{z\_uc}>$ exhibits the same frequency $1/T_M$ of the current $1/T_{HM}$ between 5 ns and 15 ns, and a double frequency between 45 ns and 55 ns, whereas in (b) it oscillates permanently at the same frequency of the current. Inset in (a): spatial distribution of the magnetization at t = 15 ns. The nanocontact and the color scale are also indicated. (Multimedia view) [URL: http://dx.doi.org/10.1063/1.4975998.1] [URL: http://dx.doi.org/10.1063/1.4975998.2] [URL: http://dx.doi.org/10.1063/1.4975998.3]

into an output voltage having the same characteristic waveform. This signal identifies the presence of the skyrmion, because, if the skyrmion was not nucleated, the $<m_{z\_uc}>$ would not show significant dynamical changes. The variation of $<m_{z\_uc}>$ is characterized by two non-stationary oscillations: one at the same frequency of the current and the other at twice such frequency. This last contribution is linked to a double passage of the skyrmion beneath the nanocontact within a period of the microwave current, and it is due to the stochasticity of thermal fluctuations, which lead the skyrmion to not deterministically cover the same trajectory in each oscillation semi-period (see also MOVIE 1 of Fig. 2 (multimedia view)). To confirm this, we carried out simulations at zero temperature, observing that $<m_{z\_uc}>$ oscillates only at the same frequency of the current (see Fig. 2(b)). For f_{HM}>0.7 GHz, the oscillatory translation of the skyrmion is too fast to obtain a robust TMR change.

As expected, the boundaries of the frequency ranges above described become larger (lower) if the current amplitude is increased (decreased), because of a faster (slower) skyrmion motion.

In the case (*ii*), we inject a perpendicular microwave current $j_{MTJ}(t) = J_{MTJ}\sin(2\pi f_{MTJ}t)$ in the MTJ with amplitude J_{MTJ} = 3 MA/cm^2 and same duration and frequency f_{MTJ} as for (*i*). Although the STT from this current acts as an anti-damping torque, it does not strongly affect the skyrmion dynamics, which, therefore, are mainly due to the thermal fluctuations in all the f_{MTJ} range. The key role is played by the Brownian diffusion that hampers the steady presence of the skyrmion under the nanocontact, resulting in non-stationary jumps of the $<m_{z\_uc}>$ (see Fig. 3(a)). Therefore, this configuration (*ii*) cannot be used for skyrmion detection.

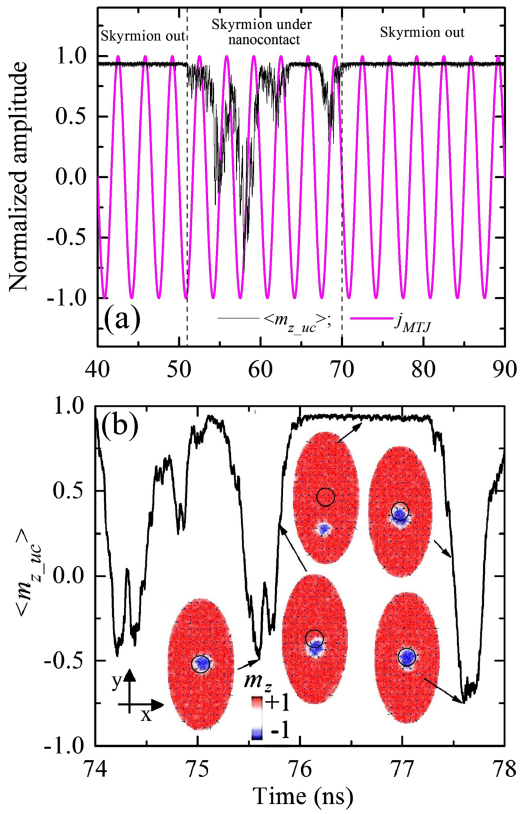

FIG. 3. (a) Temporal evolution of the normalized z-component of the magnetization under the nanocontact (black curve) and of the applied normalized microwave current (magenta curve) flowing in the MTJ only (STT), for H_{ext} = 25 mT at T = 300 K. The current amplitude and frequency are 3 MA/cm^2 and 0.3 GHz, respectively. Three regions are separated by dashed lines and refer to the position of the skyrmion with respect to the nanocontact. (b) Example of time evolution of the normalized z-component of the magnetization under the nanocontact when the SHE and STT act simultaneously, J_{HM} = 30 MA/cm^2, J_{MTJ} = 3 MA/cm^2 and same frequency of 0.3 GHz. Insets: spatial distribution of the magnetization. The nanocontact and a color scale are also indicated.

In the configuration (*iii*), we simultaneously apply both $j_{HM}(t)$ and $j_{MTJ}(t)$. We fix J_{HM} = 30 MA/cm^2 and J_{MTJ} = 3 MA/cm^2, and consider the same frequency in the range 0.1 GHz -1.0 GHz for both currents. The skyrmion dynamics, and hence, the $<m_{z\_uc}>$, exhibits similar features to the case (*i*) (frequency range to obtain TMR change, waveform, non-stationary frequency). Fig. 3(b) shows the time evolution of $<m_{z\_uc}>$, where the spatial distributions of the free layer magnetization[51] are indicated as insets and refer to the time instants pointed by the black arrows. However, we note that the presence of $j_{MTJ}(t)$ decreases the lower frequency of the range where the detection can be performed to 0.2 GHz. This is due to the local STT, which reduces the damping under the nanocontact for a certain semi-period of $j_{MTJ}(t)$, thus behaving as an "attraction pole" for the skyrmion, which is no longer expelled by the SHE.

CONCLUSIONS

In summary, we have proposed, by means of micromagnetic simulations, a method to electrically detect the presence of a Néel skyrmion in a pillar that can be easy generalized for a racetrack memory. We have considered a three-terminal device, where an MTJ is deposited on top, and, by injecting a large enough microwave current through the heavy metal layer (SHE), we are able to continuously drive the skyrmion motion under the point-contact MTJ. In this way, we critically reduce the skyrmion drift induced by thermal fluctuations at room temperature that, in absence of current, provides a stochastic drift of the skyrmion around the nanocontact (the trajectory depends on the initial seed of the thermal fluctuations). The SHE-induced skyrmion motion under the nanocontact leads to a variation of the out-of-plane component of the magnetization below the third terminal, and, consequently, of the TMR. This reading protocol can be very useful for the design of TMR read-out for the electrical detection of skyrmions.

ACKNOWLEDGMENTS

The authors thank the executive program of scientific and technological cooperation between Italy and China for the years 2016–2018 (code CN16GR09) title 'Nanoscale broadband spin-transfer-torque microwave detector' funded by Ministero degli Affari Esteri e della Cooperazione Internazionale, and Domenico Romolo for the graphical support. P. B., M. R., and R. T. also thank Fondazione Carit—Projects—'Sistemi Phased-Array Ultrasonori', and 'Sensori Spintronici'.

[1] V. S. Pribiag, I. N. Krivorotov, G. D. Fuchs, P. M. Braganca, O. Ozatay, J. C. Sankey, D. C. Ralph, and R. A. Buhrman, Nat. Phys. **3**, 498 (2007).
[2] A. Giordano, V. Puliafito, L. Torres, M. Carpentieri, B. Azzerboni, and G. Finocchio, IEEE Trans. Magn **50**, 4300404 (2014).
[3] S. Komineas, C. A. F. Vaz, J. A. C. Bland, and N. Papanicolaou, Phys. Rev. B **71**, 060405(R) (2005).
[4] V. Puliafito, L. Torres, O. Ozatay, T. Hauet, B. Azzerboni, and G. Finocchio, J. Appl. Phys. **115**, 17D139 (2014).
[5] G. Siracusano, R. Tomasello, A. Giordano, V. Puliafito, B. Azzerboni, O. Ozatay, M. Carpentieri, and G. Finocchio, Phys. Rev. Lett. **117**, 87204 (2016).
[6] N. Nagaosa and Y. Tokura, Nat. Nanotechnol. **8**, 899 (2013).
[7] J. Sampaio, V. Cros, S. Rohart, A. Thiaville, and A. Fert, Nat. Nanotechnol. **8**, 839 (2013).
[8] R. Tomasello, E. Martinez, R. Zivieri, L. Torres, M. Carpentieri, and G. Finocchio, Sci. Rep. **4**, 6784 (2014).
[9] X. Zhang, Y. Zhou, and M. Ezawa, Nat. Commun. **7**, 10293 (2016).
[10] R. H. Liu, W. L. Lim, and S. Urazhdin, Phys. Rev. Lett. **114**, 137201 (2015).
[11] Y. Zhou, E. Iacocca, A. A. Awad, R. K. Dumas, F. C. Zhang, H. B. Braun, and J. Åkerman, Nat. Commun. **6**, 8193 (2015).
[12] M. Carpentieri, R. Tomasello, R. Zivieri, and G. Finocchio, Sci. Rep. **5**, 16184 (2015).
[13] C. P. Chui and Y. Zhou, AIP Adv. **5**, 97126 (2015).
[14] G. Finocchio, M. Ricci, R. Tomasello, A. Giordano, M. Lanuzza, V. Puliafito, P. Burrascano, B. Azzerboni, and M. Carpentieri, Appl. Phys. Lett. **107**, 262401 (2015).
[15] X. Zhang, M. Ezawa, and Y. Zhou, Sci. Rep. **5**, 9400 (2015).
[16] W. Jiang, P. Upadhyaya, W. Zhang, G. Yu, M. B. Jungfleisch, F. Y. Fradin, J. E. Pearson, Y. Tserkovnyak, K. L. Wang, O. Heinonen, S. G. E. te Velthuis, and A. Hoffmann, Science **349**, 283 (2015).
[17] C. Moreau-Luchaire, C. Moutafis, N. Reyren, J. Sampaio, C. A. F. Vaz, N. Van Horne, K. Bouzehouane, K. Garcia, C. Deranlot, P. Warnicke, P. Wohlhüter, J.-M. George, M. Weigand, J. Raabe, V. Cros, and A. Fert, Nat. Nanotechnol. **11**, 444 (2016).
[18] O. Boulle, J. Vogel, H. Yang, S. Pizzini, D. de Souza Chaves, A. Locatelli, T. Sala, L. D. Buda-Prejbeanu, O. Klein, M. Belmeguenai, Y. Roussigné, A. Stashkevich, S. M. Chérif, L. Aballe, M. Foerster, M. Chshiev, S. Auffret, I. M. Miron, and G. Gaudin, Nat. Nanotechnol. **11**, 449 (2016).

[19] S. Woo, K. Litzius, B. Krüger, M.-Y. Im, L. Caretta, K. Richter, M. Mann, A. Krone, R. M. Reeve, M. Weigand, P. Agrawal, I. Lemesh, M.-A. Mawass, P. Fischer, M. Kläui, and G. S. D. Beach, Nat. Mater. **15**, 501 (2016).
[20] I. Dzyaloshinsky, J. Phys. Chem. Solids **4**, 241 (1958).
[21] T. Moriya, Phys. Rev. Lett. **4**, 4 (1960).
[22] A. Hoffmann, IEEE Trans. Magn. **49**, 5172 (2013).
[23] G. Siracusano, R. Tomasello, V. Puliafito, A. Giordano, B. Azzerboni, A. La Corte, M. Carpentieri, and G. Finocchio, J. Appl. Phys. **117**, 17E504 (2015).
[24] J. Sinova, S. O. Valenzuela, J. Wunderlich, C. H. Back, and T. Jungwirth, Rev. Mod. Phys. **87**, 1213 (2015).
[25] W. Jiang, W. Zhang, G. Yu, M. B. Jungfleisch, P. Upadhyaya, H. Somaily, J. E. Pearson, Y. Tserkovnyak, K. L. Wang, O. Heinonen, S. G. E. te Velthuis, and A. Hoffmann, AIP Adv. **6**, 55602 (2016).
[26] G. Finocchio, F. Büttner, R. Tomasello, M. Carpentieri, and M. Kläui, J. Phys. D. Appl. Phys. **49**, 423001 (2016).
[27] J. Iwasaki, M. Mochizuki, and N. Nagaosa, Nat. Nanotechnol. **8**, 742 (2013).
[28] F. Ma, M. Ezawa, and Y. Zhou, Sci. Rep. **5**, 15154 (2015).
[29] A. Giordano, R. Verba, R. Zivieri, A. Laudani, V. Puliafito, G. Gubbiotti, R. Tomasello, G. Siracusano, B. Azzerboni, M. Carpentieri, A. Slavin, and G. Finocchio, Sci. Rep. **6**, 36020 (2016).
[30] A. Neubauer, C. Pfleiderer, B. Binz, A. Rosch, R. Ritz, P. G. Niklowitz, and P. Böni, Phys. Rev. Lett. **102**, 186602 (2009).
[31] D. Liang, J. P. Degrave, M. J. Stolt, Y. Tokura, and S. Jin, Nat. Commun. **6**, 8217 (2015).
[32] X. Z. Yu, Y. Onose, N. Kanazawa, J. H. Park, J. H. Han, Y. Matsui, N. Nagaosa, and Y. Tokura, Nature **465**, 901 (2010).
[33] X. Yu, J. P. Degrave, Y. Hara, T. Hara, S. Jin, and Y. Tokura, Nano Lett. **13**, 3755 (2013).
[34] S. Heinze, K. von Bergmann, M. Menzel, J. Brede, A. Kubetzka, R. Wiesendanger, G. Bihlmayer, and S. Blügel, Nat. Phys. **7**, 713 (2011).
[35] N. Romming, C. Hanneken, M. Menzel, J. E. Bickel, B. Wolter, K. von Bergmann, A. Kubetzka, and R. Wiesendanger, Science **341**, 636 (2013).
[36] N. Romming, A. Kubetzka, C. Hanneken, K. Von Bergmann, and R. Wiesendanger, Phys. Rev. Lett. **114**, 177203 (2015).
[37] C. Hanneken, F. Otte, A. Kubetzka, B. Dupé, N. Romming, K. von Bergmann, R. Wiesendanger, and S. Heinze, Nat. Nanotechnol. **10**, 1039 (2015).
[38] C. Schutte, J. Iwasaki, A. Rosch, and N. Nagaosa, Phys. Rev. B **90**, 174434 (2014).
[39] S. Rohart, J. Miltat, and A. Thiaville, Phys. Rev. B **93**, 214412 (2016).
[40] L. Liu, C.-F. Pai, Y. Li, H. W. Tseng, D. C. Ralph, and R. A. Buhrman, Science **336**, 555 (2012).
[41] L. Liu, C. F. Pai, D. C. Ralph, and R. A. Buhrman, Phys. Rev. Lett. **109**, 186602 (2012).
[42] R. Tomasello, M. Carpentieri, and G. Finocchio, Appl. Phys. Lett. **103**, 252408 (2013).
[43] A. Giordano, G. Finocchio, L. Torres, M. Carpentieri, and B. Azzerboni, J. Appl. Phys. **111**, 07D112 (2012).
[44] G. Siracusano, A. La Corte, V. Puliafito, and G. Finocchio, J. Appl. Phys. **115**, 17D108 (2014).
[45] G. Siracusano, F. Lamonaca, R. Tomasello, F. Garescì, A. La Corte, D. L. Carnì, M. Carpentieri, D. Grimaldi, and G. Finocchio, Mech. Syst. Signal Process. **75**, 109 (2016).
[46] S. Rohart and A. Thiaville, Phys. Rev. B **88**, 184422 (2013).
[47] R. Tomasello, M. Carpentieri, and G. Finocchio, J. Appl. Phys. **115**, 17C730 (2014).
[48] G. Finocchio, V. S. Pribiag, L. Torres, R. A. Buhrman, and B. Azzerboni, Appl. Phys. Lett. **96**, 102508 (2010).
[49] J. C. Sankey, Y.-T. Cui, J. Z. Sun, J. C. Slonczewski, R. A. Buhrman, and D. C. Ralph, Nat. Phys. **4**, 67 (2007).
[50] K.-S. Ryu, S.-H. Yang, L. Thomas, and S. S. P. Parkin, Nat. Commun. **5**, 3910 (2014).
[51] L. Torres, G. Finocchio, L. Lopez-Diaz, E. Martinez, M. Carpentieri, G. Consolo, and B. Azzerboni, J. Appl. Phys. **101**, 09A502 (2007).